

# Combined Effects of Wakes and Jet Pulsing on Film Cooling

**Kristofer M. Womack**

**Ralph J. Volino**

e-mail: volino@usna.edu

Mechanical Engineering Department,  
United States Naval Academy,  
Annapolis, MD 21402

**Michael P. Schultz**

Naval Architecture and Ocean Engineering  
Department,  
United States Naval Academy,  
Annapolis, MD 21402

*Pulsed film cooling jets subject to periodic wakes were studied experimentally. The wakes were generated with a spoked wheel upstream of a flat plate. Cases with a single row of cylindrical film cooling holes inclined at 35 deg to the surface were considered at blowing ratios  $B$  of 0.50 and 1.0 with jet pulsing and wake Strouhal numbers of 0.15, 0.30, and 0.60. Wake timing was varied with respect to the pulsing. Temperature measurements were made using an infrared camera, thermocouples, and constant current (cold wire) anemometry. The local film cooling effectiveness and heat transfer coefficient were determined from the measured temperatures. Phase locked flow temperature fields were determined from cold-wire surveys. With  $B=0.5$ , wakes and pulsing both lead to a reduction in film cooling effectiveness, and the reduction is larger when wakes and pulsing are combined. With  $B=1.0$ , pulsing again causes a reduction in effectiveness, but wakes tend to counteract this effect somewhat by reducing jet lift-off. At low Strouhal numbers, wake timing had a significant effect on the instantaneous film cooling effectiveness, but wakes in general had very little effect on the time averaged effectiveness. At high Strouhal numbers, the wake effect was stronger, but the wake timing was less important. Wakes increased the heat transfer coefficient strongly and similarly in cases with and without film cooling, regardless of wake timing. Heat transfer coefficient ratios, similar to the time averaged film cooling effectiveness, did not depend strongly on wake timing for the cases considered. [DOI: 10.1115/1.2812335]*

## Introduction

Film cooling has been studied extensively to provide improved cooling of the airfoils in gas turbine engines and thus increase their life and allow for higher turbine inlet temperatures. Approximately 20–25% of compressor air is used for cooling of high performance turbine engines (Ekkad et al. [1]). If the amount of required coolant air could be reduced, engine efficiency would increase. Most investigations have focused on steady flow cases. The flow in a gas turbine engine, however, is inherently unsteady. The main flow is unsteady, with high freestream turbulence and periodic unsteadiness caused by the interaction between vane and blade rows in the turbine. Upstream airfoils shed wakes, which periodically impinge on the airfoils downstream. The wakes include a mean velocity deficit and increased turbulence, with effects similar to those of high freestream turbulence. Wakes can disrupt film cooling jets, reducing the film cooling effectiveness in some areas and possibly enhancing it in others. Wake induced turbulence may also increase heat transfer coefficients, thereby reducing the overall benefit of film cooling.

A few studies have investigated the effect of wakes on film cooling. Funazaki et al. [2,3] considered flow around the leading edge of a blunt body subject to wakes produced by a spoked wheel. In a series of studies, Ou et al. [4], Mehendale et al. [5], Jiang and Han [6], Ekkad et al. [7], Du et al. [8,9], and Teng et al. [10–12] used a linear cascade with an upstream spoked wheel to generate wakes. Film cooling effectiveness, heat transfer coefficients, and time averaged flow temperature fields were documented for cases with various blowing ratios, hole locations and geometries, density ratios, and freestream turbulence levels. Heidmann et al. [13] used a rotating facility to investigate the effect of wakes on showerhead film cooling. They report time averaged film effectiveness. Wolff et al. [14] utilized a linear cascade in a high speed facility with cooling holes on the suction side

and pressure side of their center blade. Wakes were generated with rods fastened to belts, which traveled around the cascade and two pulleys. Phase averaged velocity and turbulence levels were documented in multiple planes on both sides of the airfoil. Adami et al. [15] did numerical simulations of the flow through this cascade. Deinert and Hourmouziadis [16] conducted an experimental study in which they investigated the effects of main flow unsteadiness, but without wakes. The test surface was a flat plate, and a rotating flap downstream of the plate created the unsteadiness. Film cooling acted to suppress a separation bubble on the surface. Documentation included phase averaged velocity and temperature fields in the flow.

Further discussion of the studies listed above is available in Womack et al. [17], who documented the unsteady temperature field in a film cooling flow on a flat plate disturbed by wakes from a spoked wheel. The spokes rotated toward the plate, simulating the wake effect on an airfoil suction surface. Phase averaged temperature fields showed how the wake causes the film cooling jet to disperse. The jet returned to a steady condition between wakes at low wake Strouhal numbers, but there was insufficient time for full recovery at higher Strouhal numbers. At low blowing ratios ( $B=0.25$  and  $0.5$ ), the wakes resulted in lower film cooling effectiveness, but at a higher blowing ratio ( $B=1.0$ ), the wakes helped to mitigate jet lift-off effects by pushing the film cooling fluid back toward the wall and increasing the effectiveness. Heat transfer coefficients increased with wake passing frequency, with nearly the same percentage increase in the cases with and without film cooling. Unsteady near-wall flow temperature measurements were used to approximate the unsteady film cooling effectiveness during the wake passing cycle. During the wake passing, the unsteady effectiveness was low and approximately equal for cases at all Strouhal numbers. Variation during the rest of the cycle depended on the time available for recovery between wakes. At the lowest Strouhal number considered, the unsteady effectiveness during the wake passing dropped to less than 50% of the between wake value at some locations.

In addition to shedding wakes, airfoils passing both upstream and downstream of a turbine passage cause periodic flow blockage, inducing pressure fluctuations, which could cause film cool-

Contributed by the International Gas Turbine Institute of ASME for publication in the JOURNAL OF TURBOMACHINERY. Manuscript received June 6, 2007; final manuscript received June 22, 2007; published online August 1, 2008. Review conducted by David Wisler. Paper presented at the ASME Turbo Expo 2007: Land, Sea and Air (GT2007), Montreal, Quebec, Canada, May 14–17, 2007.

ing jets to pulsate. Only a few studies have considered the effects of pulsed jets. Bons et al. [18] used a loudspeaker to induce pulsations in their jets and examined the effects on film cooling of a flat plate. They found that pulsation resulted in reduced film cooling effectiveness for low blowing ratios, and that the effectiveness increased slightly as the blowing ratio increased to 1.5. Ligrani et al. [19], Seo et al. [20], and Jung et al. [21] used static pressure pulsations of the main flow to induce jet pulsing. They showed that pulsations cause the film cooling jet to spread more uniformly across the test surface.

Ekkad et al. [1] were the first to consider direct control of the coolant jets to improve film cooling. They controlled the pulsing using solenoid valves. Their geometry had a single film cooling hole angled at 20 deg to the surface and 90 deg to the streamwise direction, located on the leading section of a cylinder. Ekkad et al. [1] stated that pulsed jets increase the ability to effectively protect the surface and slightly lower heat transfer coefficients compared to continuous jets in some cases. Ou and Rivir [22] also found promising results in a study of shaped cooling holes using the same facility. Nikitopoulos et al. [23] did a numerical study of pulsed film cooling.

Coulthard et al. [24,25] considered pulsed film cooling from a row of holes on a flat plate. Solenoid valves were used to cyclically turn the jets on and off. Film cooling effectiveness, heat transfer coefficients, and unsteady flow temperature fields were documented. Pulsing the film coolant resulted in higher heat transfer coefficients, but the change was generally small compared to the changes in the film cooling effectiveness. Pulsing induced a high startup velocity, which momentarily increased jet lift-off. Higher pulsing frequencies tended to result in lower effectiveness. At the highest frequencies tested, however, this trend was reversed. There was insufficient time for the jets to turn fully off, resulting in some low momentum flow from the hole during the "off" portion of the cycle. At high blowing ratios, this low momentum fluid helped mitigate jet lift-off, thereby increasing the effectiveness.

Whether or not controlled pulsing can improve film cooling, natural pulsation occurs in engines and occurs in combination with wakes. To the authors' knowledge, the combined effects have not been studied in detail. The incomplete knowledge of unsteady cooling flow behavior is typically overcome by supplying enough cooling air to prevent damage to all components in the turbine. This can lead to overcooling in some areas, reducing engine efficiency. Better documentation of the unsteady behavior may lead to more efficient use of cooling air and increased engine efficiency. Given the large change in unsteady film cooling effectiveness during wake passing events documented by Womack et al. [17], the timing of pulses relative to wakes may be very important. If the pulse timing could be controlled, it might be advantageous to provide coolant only when it would be effective. Alternatively, Womack et al. [17] noted that wakes tend to mitigate jet lift-off by pushing film cooling jets back toward the surface. If wakes were timed to coincide with the start of a pulse, they might help to control the lift-off associated with startup noted by Coulthard et al. [24]. Since film cooling jets pulse in response to pressure fluctuations in engines, it might be possible through clocking to control the timing.

In the present study, the effects of pulsed jets and wakes on film cooling are combined. Experiments were conducted in a flat plate facility with a single row of five streamwise oriented round holes inclined at 35 deg to the surface and spaced  $3D$  apart. The geometry has been used in many studies including Bons et al. [18], Burd and Simon [26], Pedersen et al. [27], and Kohli and Bogard [28]. Blowing ratios of 0.5, and 1.0 were investigated with various wake passing frequencies and pulse timings relative to the wakes. In all cases, the wake passing and pulsing frequencies were equal. Phase averaged flow temperature distributions and time averaged film cooling effectiveness and heat transfer results are presented below.

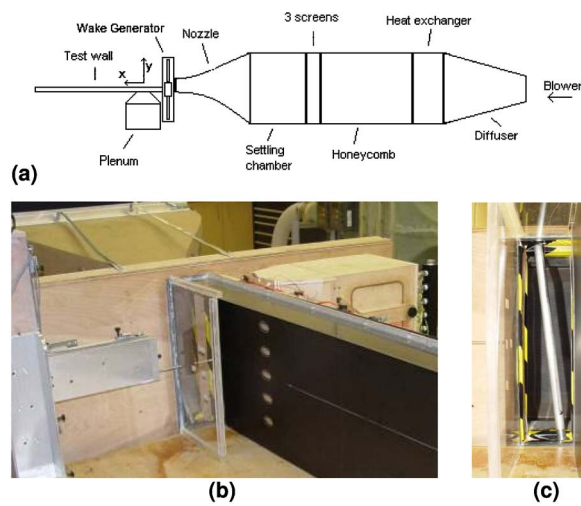


**Fig. 1 Wind tunnel configuration: (a) schematic, (b) photograph of test wall with sidewalls, (c) photograph looking upstream at rod moving across main flow**

### Experimental Facility and Measurements

Experiments were conducted in the facility constructed by Coulthard et al. [24,25,29] to study pulsing effects and modified by Womack et al. [17] to include wakes. It consists of an open loop subsonic wind tunnel with a test plate at the exit of the contraction, and a plenum to supply the film cooling jets. The wind tunnel, shown in Fig. 1, was comprised of a blower, a diffuser with three screens, a heat exchanger to maintain air nominally at 20°C, a honeycomb, a settling chamber with three screens, and a nozzle with an 8.8 area reduction. The nozzle exit area was  $0.38 \times 0.10 \text{ m}^2$ . The exiting mainstream air was uniform in temperature and velocity to within 0.1°C and 1%, respectively. The freestream turbulence intensity at the nozzle exit was 1%. This value is lower than typical intensity levels in engines. Air exiting the nozzle forms a wall jet at  $U_\infty = 8 \text{ m/s}$  along the flat plate test wall. The mainstream velocity remained at 8 m/s 18D downstream of the film cooling holes. At this downstream location, the velocity outside the boundary layer was uniform up to the edge of the free shear layer, which was located  $3D$  from the wall. The freestream unsteadiness level (rms streamwise fluctuations normalized on freestream velocity) gradually increased in the streamwise direction to 6%. This increase is due to the growth of the shear layer at the edge of the wall jet. Spectral measurements indicate that the freestream fluctuations are nearly all at frequencies between 5 Hz and 50 Hz, with a peak at 22 Hz. These low frequencies are associated with large scale structures formed in the shear layer, which buffet the boundary layer, but do not promote significant turbulent mixing. The boundary layer is therefore expected to behave as if subject to low freestream turbulence, and the heat transfer coefficient results in Coulthard et al. [29] are typical of low freestream turbulence conditions. The wall jet configuration is based on the facility of Burd and Simon [26].

The film cooling supply plenum was a box with  $0.38 \times 0.18 \times 0.36 \text{ m}^3$  inside dimensions. It was supplied by a manifold connected to a high pressure air source. The supply pressure was adjusted to vary the blowing ratio from  $B=0.5$  to 1.0. The air passed through small diameter, fast response solenoid valves (General Valve Series 9 valves with Iota 1 controllers), which choked the flow between the manifold and the plenum. For a given supply pressure, the film cooling mass flow remains constant, independent of downstream conditions. Nine valves operating in parallel provided the desired coolant mass flow. The valves could be opened for continuous blowing or set to cycle between fully open and fully closed positions. In the present pulsed cases,

they were set for a 50% duty cycle, i.e., the valves were open and closed for equal intervals during the jet pulsing cycle. The plenum contained a finned tube heat exchanger, midway between the valves and the film cooling holes. Warm water at 30°C circulated through the tubes, heating the air to approximately 27°C. Details of the capacitance of the plenum and the response of the film cooling jets to the valve actuation are available in Coulthard et al. [24].

The test wall was constructed of polyurethane foam with a thermal conductivity of 0.03 W/mK. The dimensions were 0.38 m wide, 44 mm thick, and 1.17 m long, with a starting length of 13.3*D* upstream of the row of film cooling holes. A wall opposite the starting length and sidewalls along the length of the test wall, as shown in Fig. 1(b), helped limit interaction between the wind tunnel flow and the still air in the room. Foil heating elements were placed on the foam surface to provide a uniform heat flux condition, and are described in more details in Coulthard et al. [25,29]. Heaters were located both upstream and downstream of the film cooling holes. The heaters were covered with a 0.79 mm thick sheet of black Formica® laminate to provide a smooth test surface. The film cooling geometry consisted of a single row of five round holes inclined at 35 deg to the surface. The sharp edged holes had a diameter of  $D=19.05$  mm, a length to diameter ratio  $L/D=4$ , and were spaced  $3D$  apart, center to center. A 1.6 mm thick trip was installed  $11D$  upstream of the leading edge of the film cooling holes, producing a fully turbulent boundary layer.

Wakes were generated with a spoked wheel between the contraction and the test plate. The hub of the wheel was driven by an electric motor and had 24 threaded holes around its circumference, into which 38 cm long, 1.905 cm diameter hollow aluminum rods could be installed. When the hub was rotated, the rods cut through the main flow, generating wakes. The rods were intended to produce wakes simulating those shed from the trailing edges of upstream airfoils. In an engine, the diameter of an airfoil trailing edge is of the same order as the diameter of typical film cooling holes. The rods in the present study, therefore, were chosen to have the same diameter as the film cooling holes in the test plate. The wake passing velocity in a turbine is of the same order as the main flow velocity, so the rotation speed of the spoked wheel was set at 200 rpm, which produced rod velocities of 8 m/s at the spanwise centerline of the test section. Combinations of 3, 6, and 12 rods were used to produce wake passing frequencies of 10 Hz, 20 Hz, and 40 Hz. When nondimensionalized using the rod diameter and main flow velocity, these frequencies correspond to Strouhal numbers,  $Sr=2\pi fD/U_\infty$ , of 0.15, 0.30, and 0.60. These  $Sr$  are typical of engine conditions and match the range considered by Heidmann et al. [13]. The direction of rotation was set so that the rods moved toward the test plate (clockwise when looking upstream in Figs. 1(b) and 1(c)), to simulate wakes impacting the suction side of an airfoil. Further details of the wake generator are available in Womack et al. [17].

**Measurements.** Thermocouples were placed in the film cooling plenum, at the plenum-side end of the outermost film cooling hole, at the wind tunnel exit, on the back of the test plate, in the ambient air, on the wall of the room to measure the surrounding temperature for radiation corrections, and in ice water as a reference. Constant current (cold-wire) and constant temperature (hot-wire) anemometry were used to measure flow temperature and velocity, respectively. Boundary layer probes with 1.27  $\mu\text{m}$  diameter platinum sensors (TSI model 1261A-P.5) were used for temperature measurements, and boundary layer probes with 3.81  $\mu\text{m}$  diameter tungsten sensors (TSI model 1218-T1.5) were used for the velocity. An infrared (IR) camera (FLIR Systems Merlin model) with a Stirling cooled detector was used to measure the surface temperature field of the test wall. The temperature resolution of the camera was 0.05°C. The camera had a 255  $\times$  318 pixel detector and was positioned such that each pixel corresponded to a 1  $\times$  1 mm<sup>2</sup> area on the test wall. The field of view

on the test wall corresponded to  $13.4D \times 16.7D$ .

An infrared sensor was used to detect the passing of the wake generator rods. The pulse train from this sensor was digitized along with the instantaneous anemometer voltages (typically 13 s long traces at a 10 kHz sampling rate) to allow phase averaging of the flow velocities and temperatures relative to the wake passing events. Phase averaged results were typically computed at 24 increments during the wake passing cycle. The pulse train from the sensor was also used as the input to a circuit, which controlled the valves for cases with pulsed jets and wakes. The delay between the wake passing and pulse start, and the duration of the pulse were independently adjustable.

The film cooling effectiveness and Stanton number were defined, respectively, as follows:

$$\eta = \frac{T_{aw} - T_\infty}{T_{jet} - T_\infty} \quad (1)$$

$$St = \frac{q''_{conv}}{\rho c_p U_\infty (T_w - T_{aw})} \quad (2)$$

The jet, freestream, and wall ( $T_w$ ) temperatures were measured. The convective heat flux  $q''_{conv}$  was determined based on the power input to the heaters, with corrections for conduction and radiation losses. Measurements were made for each flow condition with the wall heaters on and off, to determine local  $T_{aw}$ ,  $\eta$ , and  $St$ . The procedure is described in more details in Coulthard et al. [25]. Stanton numbers were determined for cases with film cooling ( $St_f$ ), and in cases without film cooling ( $St_o$ ) but otherwise similar main flow, wake, and surface heating conditions. Stanton number ratios ( $St_f/St_o$ ) were computed to determine the effect of film cooling on heat transfer coefficients.

The thermocouples and IR camera were calibrated against a precision blackbody source, and the cold-wire probe was calibrated against the thermocouples. The uncertainty in the measured temperature is 0.2°C, and the uncertainty in the measured velocity is 3%. The uncertainty in the film cooling effectiveness was determined to be 6% and the uncertainty in the Stanton number is 8%. The uncertainty in the ratio of two Stanton numbers is 11%, based on a standard propagation of error with a 95% confidence interval.

As documented in Coulthard et al. [25] before installation of the wake generator, the boundary layer  $0.8D$  upstream of the film cooling hole leading edge had a momentum thickness Reynolds number of 550 and a shape factor of 1.48. The local skin friction coefficient at this location was  $5.4 \times 10^{-3}$  and the enthalpy thickness Reynolds number was 470. The Reynolds number based on hole diameter and mainstream velocity was 10,000. Womack et al. [17] confirmed that with the wake generator operating at low  $Sr$ , the phase averaged velocity profile between wakes matched the profile acquired before installation of the wake generator.

As shown in Womack et al. [17], the freestream turbulence level rose from about 1% between wakes to about 19% in the wakes. For the  $Sr=0.15$  case, the freestream settled to its undisturbed state between wakes, and this undisturbed condition occupied about 60% of the cycle. The influence of the wake on the turbulence extended all the way to the wall. When the leading edge of the wake arrived at the hole, the freestream turbulence level rose sharply. About 5 ms later, a similar rise in turbulence was observed near the wall. About 15 ms later, the near-wall turbulence level had fallen. About 20 ms after this, the freestream turbulence level returned to its undisturbed condition. The duration of the wake, therefore, was about 40 ms in the freestream, with the strongest near-wall influence lasting about 15 ms. At the higher Strouhal numbers, the dimensional timing of the wakes was about the same, since the freestream velocity and wake generator speed were unchanged. The time between wakes was reduced, however, so the disturbed flow occupied a larger fraction of the cycle. At  $Sr=0.3$ , the calm flow between wakes occupied

**Table 1 Naming convention for pulse/wake combinations**

| Name | Description                                       |
|------|---------------------------------------------------|
| P/NW | Pulsed jets, No wakes (steady freestream)         |
| P/WO | Pulsed jets, wakes impact out of (between) pulses |
| P/WI | Pulsed jets, wakes impact In (during) pulses      |
| S/W  | Steady jets with wakes                            |
| S/NW | Steady jets, no wakes (steady freestream)         |

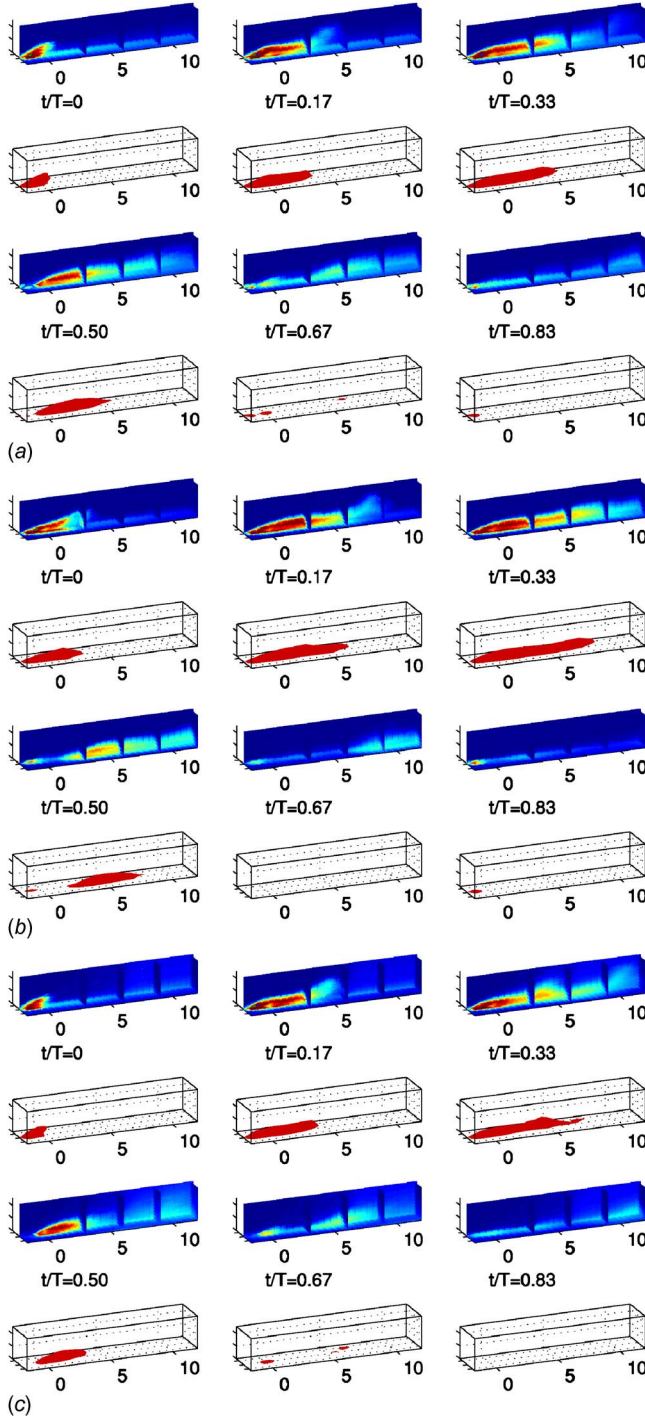


**Fig. 2 Dimensionless temperature field,  $\phi$ , for  $B=0.5$ ,  $Sr=0.15$ , upper image shows temperature contours in various planes, color range 0 (blue) to 0.6 (red); lower image shows isothermal surface with  $\phi=0.3$ ; axis limits:  $x=-1.74D$  to  $12D$ ,  $z=-1.5D$  to  $1.5D$ ,  $y=0$  to  $2.55D$ ; (a) P/NW, (b) P/WO, (c) P/WI (see Table 1 for names)**

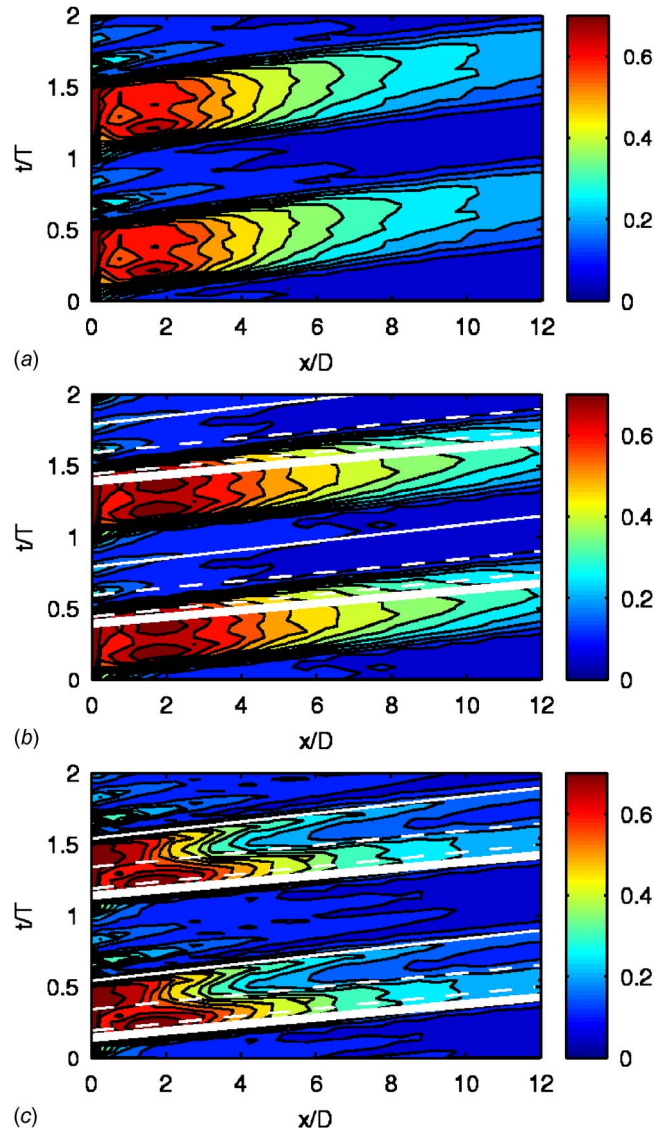


**Fig. 3 Phase averaged  $\eta^*$  for  $B=0.5$ ,  $Sr=0.15$ , white lines indicate wake duration in freestream (solid) and near-wall (dashed); (a) P/NW, (b) P/WO, (c) P/WI**

about 20% of the cycle. At  $Sr=0.6$ , the wakes merged, and the freestream turbulence level cycled between a low of about 10% and a high of 19%.

Velocity profiles acquired at multiple streamwise locations showed that the propagation speed of the leading edge of the wake was about equal to the undisturbed freestream velocity,  $U_\infty = 8$  m/s. The trailing edge of the wake was somewhat slower, at about  $0.8U_\infty$ . Near the wall, the leading and trailing edges of the disturbed flow traveled at about  $0.9U_\infty$ . Further details of the wake including velocity and turbulence profiles are available in Womack et al. [17].

The film cooling jet velocity and temperature distributions at the hole exit plane were documented in Coulthard et al. [24]. The jet temperature was very uniform and matched the plenum temperature to within  $0.2^\circ\text{C}$ . With steady blowing, the velocity was highest in the upstream section of the hole, and agreed with the results of Burd and Simon [26], who considered the same geometry. Phase averaged velocity distributions were also shown in Coulthard et al. [24]. Since the jets were only heated to approximately  $7^\circ\text{C}$  above the mainstream temperature, the density ratio of jets to mainstream was 0.98. Hence the blowing and velocity

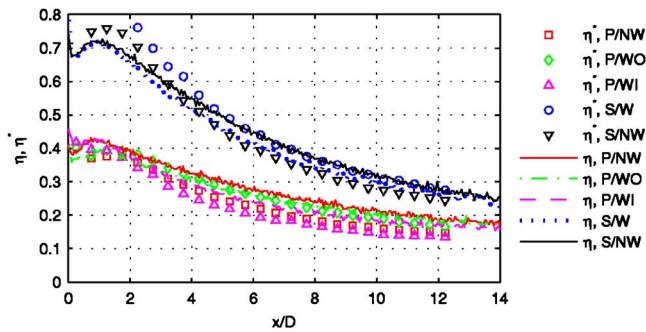


Fig. 4 Time averaged centerline  $\eta$  and  $\eta^*$  for  $B=0.5$ ,  $Sr=0.15$

ratios were essentially equal.

Three-dimensional surveys of the flow temperature were measured using the cold-wire probe. Each survey consisted of a  $29 \times 11 \times 5$  grid with 1595 measurement locations. In the streamwise direction, 29 evenly spaced locations extended from  $x=-1.74D$  (the leading edge of the film cooling holes) to  $12.2D$ . In the wall normal direction, there were 11 evenly spaced locations extending from  $y=0$  to  $2.55D$ . Coulthard et al. [24] confirmed that the flow was symmetric about the spanwise centerline in this facility, so spanwise locations were all on one side of the centerline, with five evenly spaced points extending from  $z=0$  to the midpoint between adjacent holes at  $z=1.5D$ .

## Results and Discussion

### $B=0.5$ Cases

$Sr=0.15$ . The nominal blowing ratio in the discussion below refers to the blowing rate when the jets are turned on. For the pulsed cases, this means the time averaged blowing ratio is about

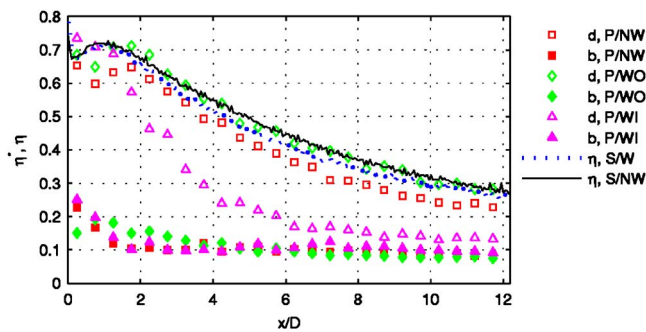


Fig. 5 Phase averaged centerline  $\eta^*$  for  $B=0.5$ ,  $Sr=0.15$ ,  $d$  =during pulse,  $b$ =between pulses

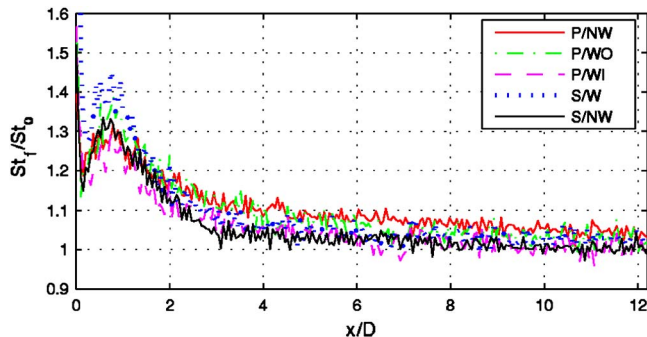
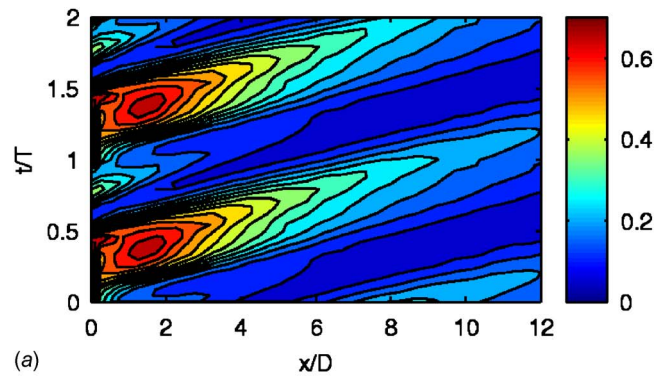
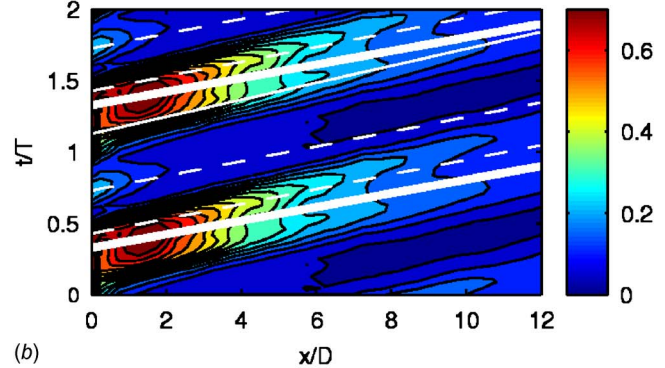


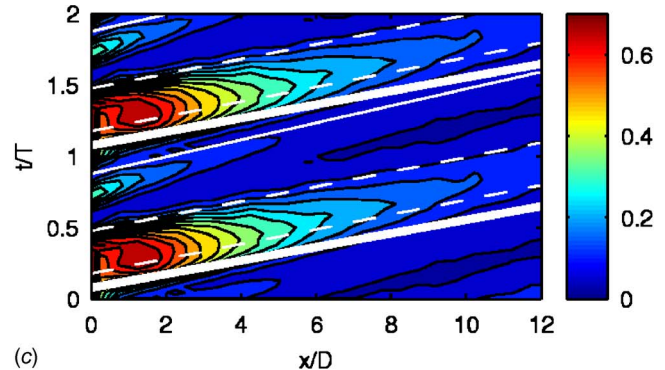
Fig. 6 Centerline Stanton number ratio,  $St_t/St_0$ , for  $B=0.5$ ,  $Sr=0.15$



(a)



(b)



(c)

Fig. 7 Phase averaged  $\eta^*$  for  $B=0.5$ ,  $Sr=0.30$ ; (a) P/NW, (b) P/WO, (c) P/WI

0.25 for the nominal  $B=0.5$  cases. Various pulsing/wake combinations were tested for each blowing ratio as described by the naming convention in Table 1. The three-dimensional temperature fields for the nominal  $B=0.5$  cases with Strouhal number equal 0.15 are shown in Fig. 2. Six phases of the jet pulsing cycle are shown for each case, labeled with the time  $t$  normalized on the

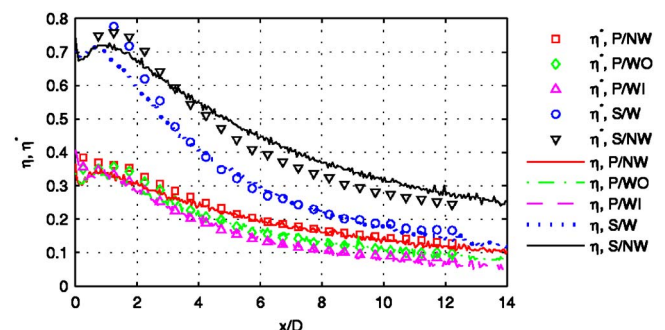


Fig. 8 Time averaged centerline  $\eta$  and  $\eta^*$  for  $B=0.5$ ,  $Sr=0.30$

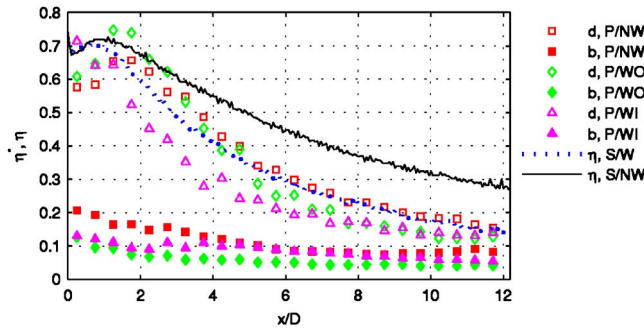


Fig. 9 Phase averaged centerline  $\eta^*$  for  $B=0.5$ ,  $Sr=0.30$

period  $T$ . As explained in Coulthard et al. [24], the plenum dynamics result in about a 4 ms delay between the opening of the solenoid valves and the first appearance of the jet at the hole exit plane. Another 10 ms elapses before the jet is of sufficient strength for significant coolant to be observed at the trailing edge of the hole. This delay is accounted for in all the figures that follow, so  $t/T=0$  corresponds to the arrival of the jet at  $x=0$ . The top image at each phase shows dimensionless temperature contours,  $\phi=(T-T_\infty)/(T_{jet}-T_\infty)$ , in multiple planes arranged to provide a three-dimensional image of the temperature field. The color range is from  $\phi=0$  (blue) to  $\phi=0.6$  (red), and the axes extend from  $-1.74D$  to  $12D$  in the streamwise direction,  $-1.5D$  to  $1.5D$  in the spanwise direction, and 0 to  $2.55D$  in the wall normal direction. The lower image in each figure shows an isothermal surface with  $\phi=0.3$ . This value of  $\phi$  was found to give a good visual representation of the jet position. The axis limits are the same as in the upper figure. Some of the axis labels have been removed to unclutter the figures. Figure 2(a) shows the case with pulsed jets and a steady freestream. The jet is emerging from the hole at  $t/T=0$  and shows some signs of lift-off. The lift-off does not continue beyond the startup, and in the next two frames, the jet is near the wall as its extent increases along the surface. At  $t/T=0.5$  the jet has turned off, and the coolant convects downstream and out of the field of view in the next two frames. The pulsing is the same in Fig. 2(b), but a wake arrives at the hole at  $t/T=0.39$ . The wake has been timed to largely miss the jet pulse. Comparing Figs. 2(a) and 2(b), there is little difference at the first three phases, as expected since the wake is not yet present. The wake does appear to increase the dispersal of the jet somewhat at  $t/T=0.5$  and 0.67, but by this point there is little jet fluid present and the film cooling effectiveness will already be low even without the wake. In Fig. 2(c), the wake is timed to disrupt the jet pulse and arrives at the hole at  $t/T=0.14$ . Comparing Figs. 2(a) and 2(c), it appears that the jet has been disrupted somewhat be-

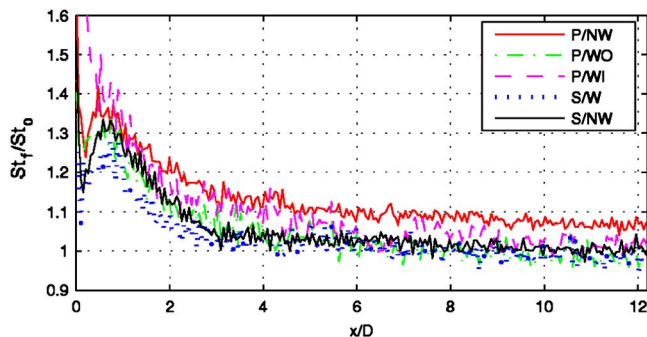


Fig. 10 Centerline Stanton number ratio,  $St_f/St_0$ , for  $B=0.5$ ,  $Sr=0.30$

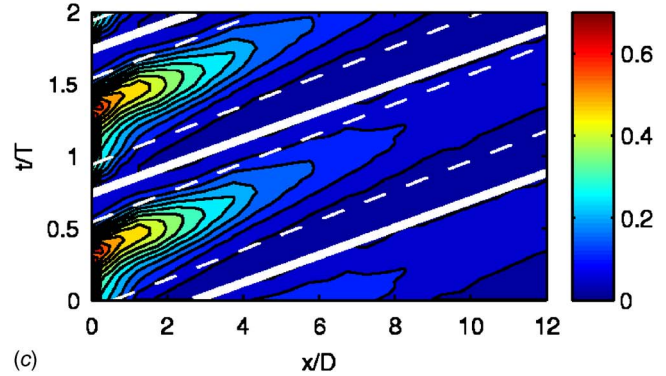
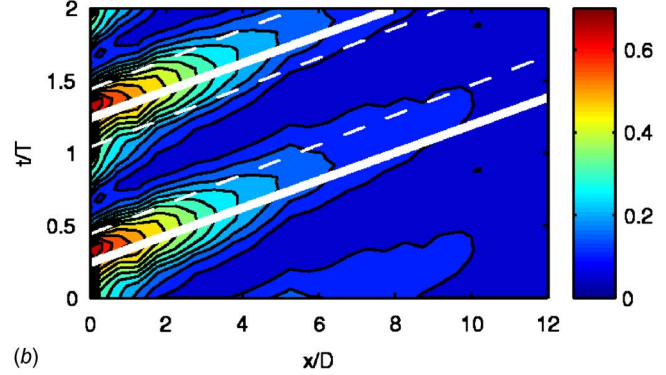
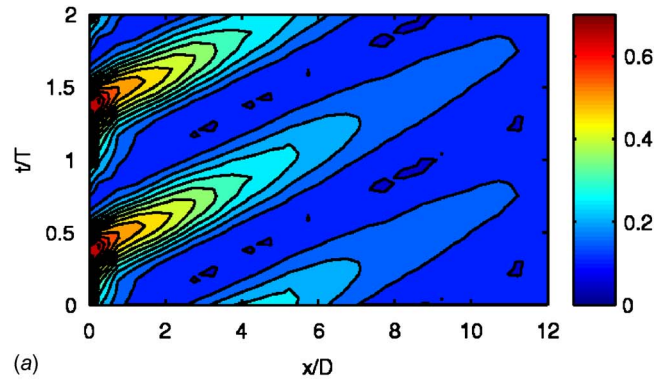


Fig. 11 Phase averaged  $\eta^*$  for  $B=0.5$ ,  $Sr=0.60$ ; (a) P/NW, (b) P/WO, (c) P/WI

tween  $t/T=0.17$  and 0.50.

Womack et al. [17] defined an approximate unsteady film cooling effectiveness,

$$\eta^* = \phi(y=0.08D) = \frac{T(y=0.08D) - T_\infty}{T_{jet} - T_\infty} \quad (3)$$

based on the near-wall phase averaged flow temperature at  $y/D=0.08$ . Womack et al. [17] found that time averaged  $\eta^*$  agreed very closely with  $\eta$  based on surface temperature measurements, in agreement with Kohli and Bogard [28] who showed that the time averaged flow temperature at  $y/D=0.1$  agreed with the wall temperature to within 0.02 in  $\phi$ . Because of the thermal mass of the wall, its surface temperature cannot respond rapidly enough to follow the fluctuations induced by pulsing or wakes. The flow temperature above the wall does respond rapidly, however, so phase averaged  $\eta^*$  provides an estimate of the instantaneous film cooling effectiveness during the wake and pulsing cycles. Figure 3 shows phase averaged  $\eta^*$  from the spanwise centerline on a time-space plot for the cases of Fig. 2. The vertical axis indicates the phase, with the data repeated to show 2 cycles. A horizontal line on the figure shows the value of  $\eta^*$  at a particular phase. The

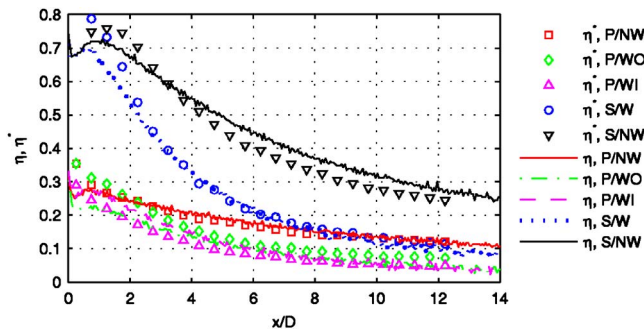


Fig. 12 Time averaged centerline  $\eta$  and  $\eta^*$  for  $B=0.5$ ,  $Sr=0.60$

white lines in Figs. 3(b) and 3(c) show the location of the wake. The thicker solid line corresponds to the leading edge of the wake in the freestream, and the thinner solid line indicates the trailing edge in the freestream. The dashed lines indicate the leading and trailing edges of the period of strong wake turbulence near the wall. The effect of the pulsing is clear. The effectiveness is high during the pulse and drops to near zero between pulses. In Fig. 3(b), the wake lies largely between pulses and appears to have little effect on the film cooling. In Fig. 3(c), the wake cuts through the pulse and appears to have a large effect in reducing the effectiveness.

The actual centerline effectiveness  $\eta$  along with the time averaged  $\eta^*$  is shown for all the  $B=0.5$ ,  $Sr=0.15$  cases in Fig. 4. Included are cases with and without wakes, with steady and pulsed jets, and also the steady  $B=0.5$  case without wakes for comparison. The agreement between  $\eta$  and  $\eta^*$  is good in all cases, and is within the experimental uncertainty at most locations. Pulsing has a large impact in lowering the effectiveness, as shown in Coulthard et al. [24]. This is expected since the coolant mass flow is reduced by a factor of 2 and the effectiveness between pulses is near zero, as shown in Fig. 3. The wakes appear to have only a small effect on  $\eta$ , in agreement with the results of Womack et al. [17] at this Strouhal number. The case with the seemingly large disruption of the jet shown in Fig. 2(c) (P/WI in Fig. 4) does have the lowest  $\eta$ , but it is only slightly lower than the other pulsed cases.

Figure 5 shows  $\eta^*$  for the cases of Fig. 4 at particular phases either during (d) or between (b) pulses. These data were extracted from Fig. 3 along diagonal lines with slopes corresponding to the convection velocity. Also shown for reference in Fig. 5 are the corresponding steady blowing cases with and without wakes. Between pulses,  $\eta^*$  is near zero. It is not exactly zero, however, since the near-wall fluid is heated by the wall between pulses, making  $\eta^*$  only an approximation to the instantaneous adiabatic effectiveness. For the P/NW and P/WO cases, the effectiveness during the pulse is about equal to  $\eta$  for the steady blowing cases.

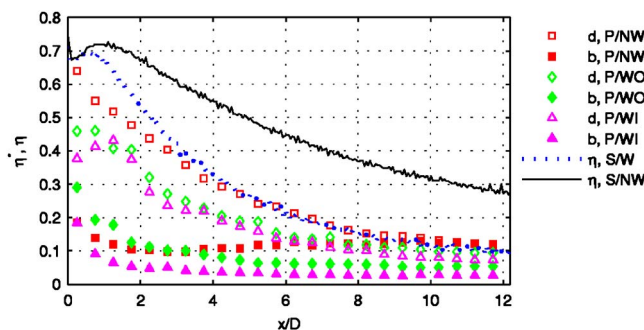


Fig. 13 Phase averaged centerline  $\eta^*$  for  $B=0.5$ ,  $Sr=0.60$

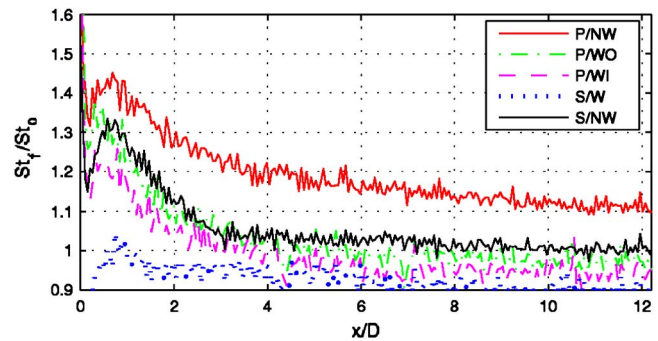


Fig. 14 Centerline Stanton number ratio,  $St_f/St_o$ , for  $B=0.5$ ,  $Sr=0.60$

The effectiveness during the pulse for the P/WI case, however, is reduced by about 50% when the wake impacts. Depending on its timing, the wake can have a large role in disrupting the film cooling flow and reducing the instantaneous effectiveness, but for the  $Sr=0.15$  cases, this disruption occupies a relatively small fraction of the cycle, so the overall impact on  $\eta$  is small.

Figure 6 shows the centerline Stanton number ratio,  $St_f/St_o$ , for the  $B=0.5$ ,  $Sr=0.15$  cases. Womack et al. [17] showed that wakes significantly increase the Stanton number, but the relative percentage increase is nearly the same with and without film cooling. Hence,  $St_f$  and  $St_o$  both increase such that the ratio  $St_f/St_o$  is about the same with and without wakes. This is seen in Fig. 6, where all cases agree with each other and wake timing does not play a noticeable role. Film cooling causes a rise in Stanton number just downstream of the holes, which drops off a few diameters downstream. More discussion of this Stanton number behavior is available in Coulthard et al. [25,29].

Spanwise averaged results show the same trends as the centerline data of Figs. 3–6 and are not included in the present paper. Spanwise averaged results are included in Coulthard et al. [24,25] and Womack et al. [17] for the cases with separate pulsing and wakes. As discussed below for the centerline data, the separate effects of pulsing and wakes are additive, and the same is true for the spanwise averaged results.

$Sr=0.30$ . Figures 7–10 show results for the  $B=0.5$ ,  $Sr=0.3$  cases in the format of Figs. 3–6. Comparison of the time-space plots in Figs. 7(a) and 7(c) shows reduction of the effectiveness by the wake. The effect is actually stronger than in the  $Sr=0.15$  case of Fig. 3(c), but is less distinct because the wake is spread over a larger fraction of the cycle in Fig. 7(c). Figure 8 shows time averaged  $\eta$  and  $\eta^*$ , which again agree very well with each other. Wakes with  $Sr=0.3$  reduce the effectiveness by 30–50% for the steady blowing case, which is more significant than the small change observed for the  $Sr=0.15$  cases of Fig. 4. Pulsing alone reduces  $\eta$  by a factor of about 2 compared to the steady blowing case. Combined pulsing and wakes reduce the effectiveness by about 65–75%, which suggests that the individual effects of pulsing and wakes are additive (i.e., if pulsing reduces  $\eta$  to 0.5 its steady value and wakes reduce the 0.5 another 30% to 0.35, then the combined effect is a 65% reduction below the S/NW case). The same additive behavior was observed in all cases. The P/WI case has the lowest  $\eta$ , as expected, although the differences in  $\eta$  with different wake timings are within the uncertainty. Figure 9 shows the phase averaged  $\eta^*$  during and between pulses. As in the  $Sr=0.15$  case, the effectiveness is near zero between pulses. During the pulses,  $\eta^*$  never achieves the steady freestream value, even in the P/NW case, in contrast to the  $Sr=0.15$  results. The P/WI case had the lowest  $\eta^*$  during pulses, as expected, but the difference between timings was lower than in the  $Sr=0.15$  case. The higher Strouhal number results in less recovery time between wakes, so the jet never fully reaches steady conditions. Some

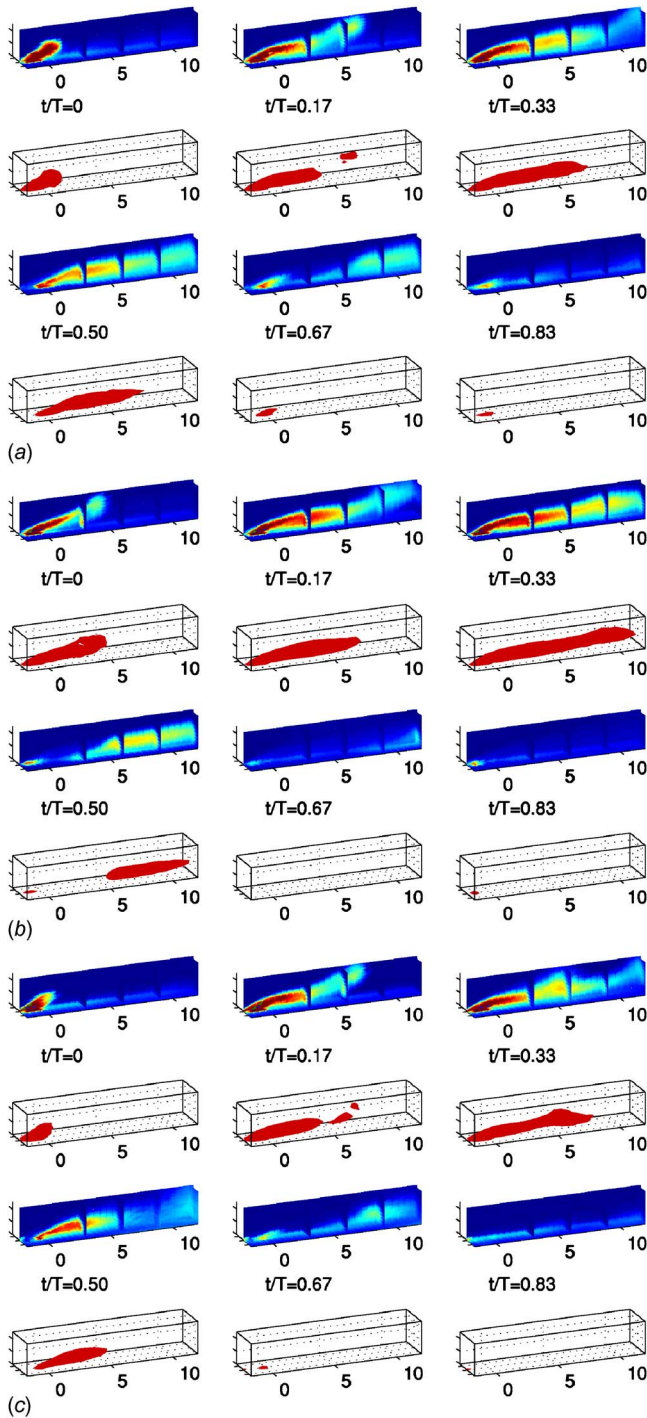


Fig. 15 Dimensionless temperature field,  $\phi$  for  $B=1.0$ ,  $Sr=0.15$ ; (a) P/NW, (b) P/WO, (c) P/WI

disturbance is present for most of the cycle, regardless of wake timing, so the distinction between the various timings is also reduced. The Stanton number ratio for the  $B=0.5$ ,  $Sr=0.3$  cases are shown in Fig. 10. As at  $Sr=0.15$ , the difference between cases is small.

$Sr=0.60$ . The  $B=0.5$ ,  $Sr=0.6$  case results are shown in Figs. 11–14. Pulsing results in jet lift-off during the startup of each pulse, and for the  $Sr=0.6$  cases, the startup period occupies a large fraction of the pulse. This is seen in the time-space plots of Fig. 11 as reduced effectiveness during most of the pulse, followed by a short period of higher  $\eta^*$  just as the jet turns off. The thin white

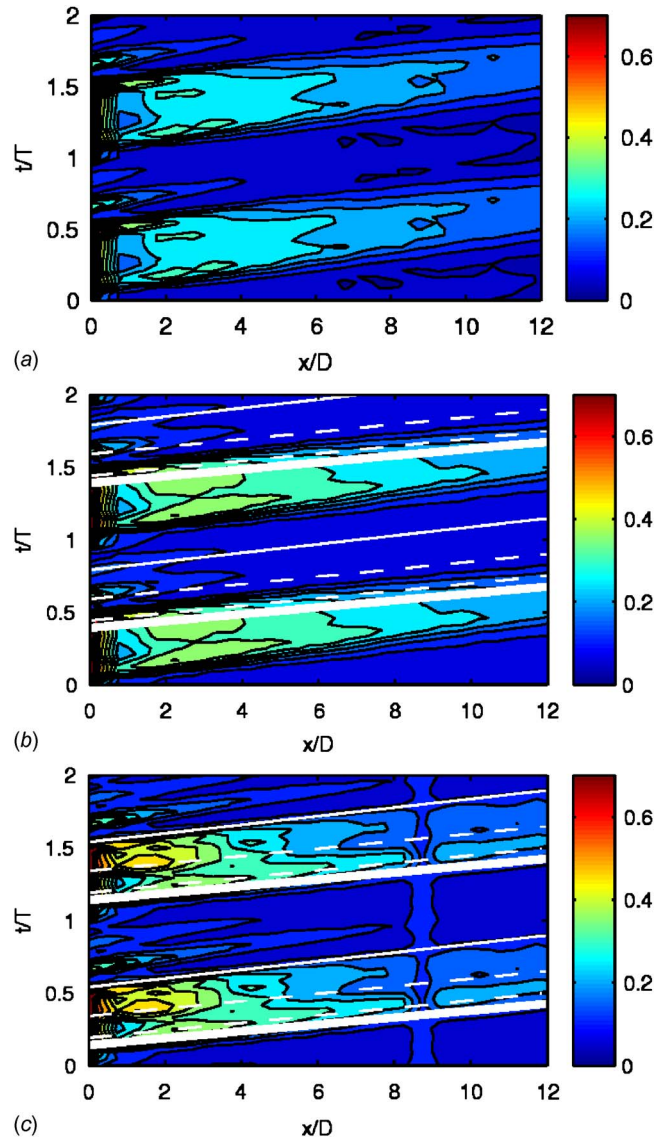


Fig. 16 Phase averaged  $\eta^*$  for  $B=1.0$ ,  $Sr=0.15$ ; (a) P/NW, (b) P/WO, (c) P/WI

line indicating the trailing edge of the wake is not shown in Fig. 11 since the wakes overlap each other. The wakes reduce the effectiveness, but the timing does not appear to matter. Since the wake disturbance occupies the full pulsing cycle, little variation with timing should be expected. Figure 12 shows that pulsing alone reduces  $\eta$  by about 60% (due to the combined effects of lower coolant mass flow and increased lift-off), and wakes alone reduce  $\eta$  by 60% or more, particularly at downstream locations. The combined effects are commensurate with the individual reductions. Effectiveness in the P/WI case was reduced by as much as 85% from the steady blowing case without wakes. Figure 13 shows the phase averaged  $\eta^*$  during and between pulses. As in the lower  $Sr$  cases,  $\eta^*$  is low between pulses, as expected. During pulses, the effectiveness is much lower than in the steady blowing case, even without wakes, due to jet lift-off during pulse startup. Wakes reduce  $\eta^*$  further, and again the results are about equal for the two wake timings. Stanton number ratios for the  $B=0.5$ ,  $Sr=0.6$  cases are shown in Fig. 14. Most of the cases agree with each other and are about equal to those at the lower  $Sr$  in Figs. 6 and 10. Wake timing effects again appears insignificant. The Stanton ratios for the P/NW case are noticeably higher than those of the other cases. Pulsing raises Stanton numbers, but the effect is

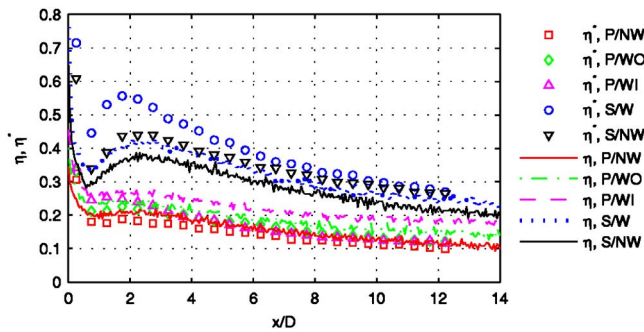


Fig. 17 Time averaged centerline  $\eta$  and  $\eta^*$  for  $B=1.0$ ,  $Sr=0.15$

relatively small in comparison with the effect of the wakes. Since the wake effect is present in both  $St_f$  and  $St_o$ , the pulsing effect is less apparent in the ratios for the cases with wakes.

#### $B=1.0$ Cases

$Sr=0.15$ . Figure 15 shows phase averaged temperature fields for the  $B=1.0$ ,  $Sr=0.15$  cases in the same format as Fig. 2. With higher mass flow, the jets extend farther down the surface before being dispersed than in the lower  $B$  cases, but there is also more jet lift-off and, therefore, less coolant near the wall. The wake timings are the same as in Fig. 2. The wake disturbs the jet at  $t/T=0.5$  and  $t/T=0.67$  in Fig. 15(b), and at  $t/T=0.17-0.5$  in Fig. 15(c). The near-wall effect of this is shown in the time-space plots of Fig. 16. Effectiveness is lower than in the  $B=0.5$  case of Fig. 3 due to lift-off, which is particularly apparent at  $x/D < 1$ . When the wakes pass during the pulses, they momentarily increase  $\eta^*$  in the upstream region by suppressing lift-off. The wake effect farther downstream appears slight, since the jet fluid is largely away from the wall and dispersed even without wakes. Figure 17 shows that the time averaged effectiveness drops by about 50% between the steady and pulsed jets, as expected with the 50% mass flow reduction. Wakes raise the effectiveness slightly both with steady and pulsed jets, and this rise is slightly larger for the P/WI case. The differences with wakes are small, however, and within the experimental uncertainty. The phase averaged  $\eta^*$  results of Fig. 18 show that the effectiveness is low between jet pulses, and approaches the steady blowing results during the pulses, in agreement with the  $B=0.5$  results in Fig. 5. The wake enhances  $\eta^*$  at  $x/D < 2$  by reducing lift-off, but has little effect farther downstream. Stanton number ratios for the  $B=1.0$ ,  $Sr=0.15$  cases are shown in Fig. 19. All agree with each other, as in the  $B=0.5$  cases.

$Sr=0.30$  and  $0.60$ . Figures 20–23 show results for the  $B=1.0$ ,  $Sr=0.3$  cases and Figs. 24–27 are for the  $B=1.0$ ,  $Sr=0.6$  cases. As in the  $B=1.0$ ,  $Sr=0.15$  cases, during the pulses the wakes tend to increase effectiveness upstream of  $x/D=2$ , particularly in the

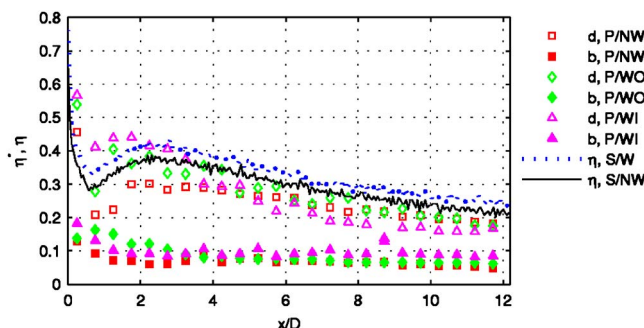


Fig. 18 Phase averaged centerline  $\eta^*$  for  $B=1.0$ ,  $Sr=0.15$

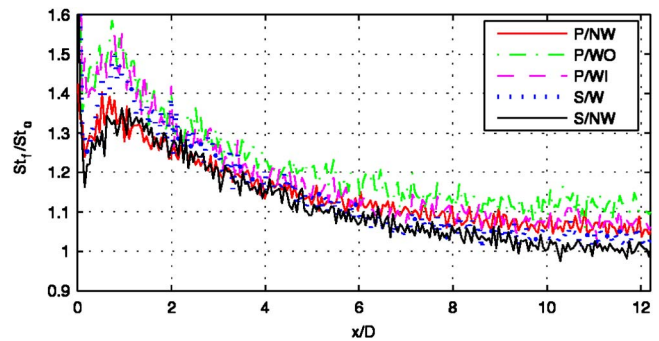


Fig. 19 Centerline Stanton number ratio,  $St_f/St_o$ , for  $B=1.0$ ,  $Sr=0.15$

P/WI case, and reduce effectiveness farther downstream. The time averaged results show that the wake effect is relatively small. Stanton number ratios show no significant differences with wake timing, but the ratios are about 10% higher for the P/NW cases.

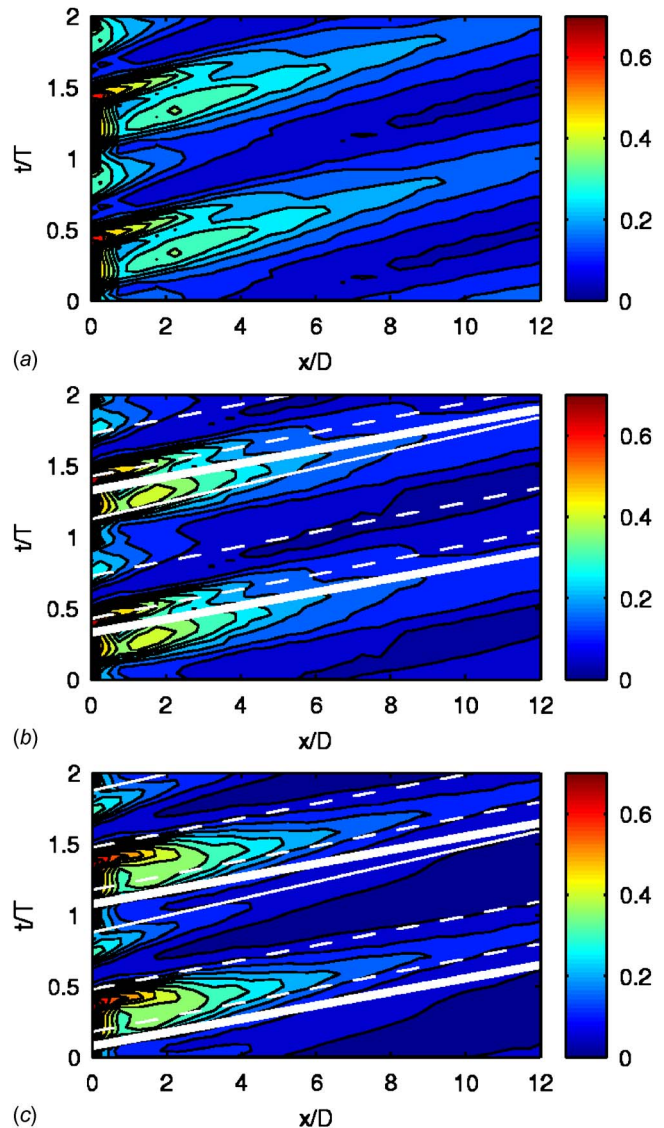


Fig. 20 Phase averaged  $\eta^*$  for  $B=1.0$ ,  $Sr=0.30$ ; (a) P/NW, (b) P/WO, (c) P/WI

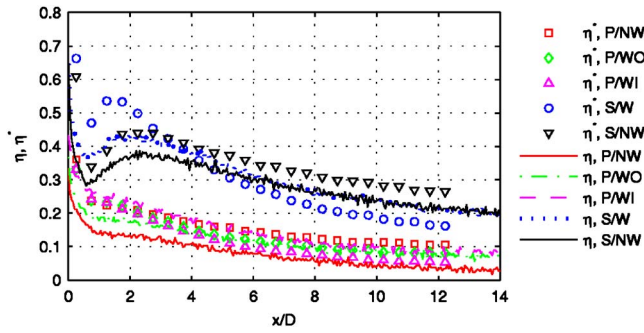


Fig. 21 Time averaged centerline  $\eta$  and  $\eta^*$  for  $B=1.0$ ,  $Sr=0.30$

As in the  $B=0.5$  case of Fig. 14, pulsing increases Stanton numbers, but the effect is hidden by the larger wake effect in the cases with wakes.

It should be noted that wakes increase the lateral spreading of the film cooling jets. When combined with a reduction in lift-off, this results in a significant increase in the spanwise averaged effectiveness in the  $B=1.0$  cases, as shown in Womack et al. [17]. The wakes, therefore, help to mitigate the reduction in  $\eta$  caused by pulsing. As noted above, the pulsing and wake effects are additive, so the combined effects on the spanwise averaged data can be deduced from the separate effects presented in Coulthard et al. [24] and Womack et al. [17]. Direct measurements of the combined effects show that wake timing has little effect on the spanwise averaged results, in agreement with the centerline results discussed above.

### Conclusions

With  $B=0.5$ , film cooling jet pulsing and passing wakes both act to reduce the film cooling effectiveness. In combination, the reduction in effectiveness is greater than with either effect alone.

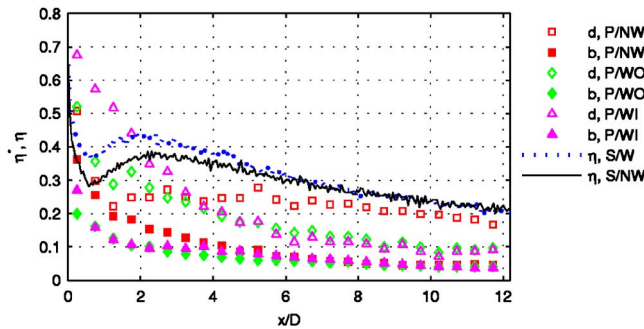


Fig. 22 Phase averaged centerline  $\eta^*$  for  $B=1.0$ ,  $Sr=0.30$

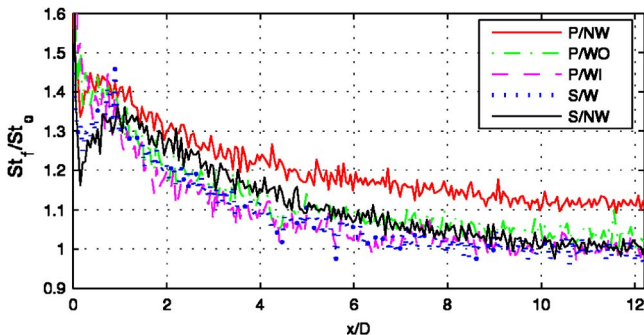
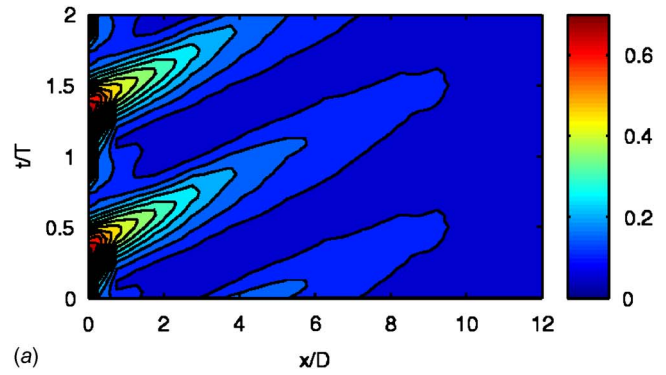
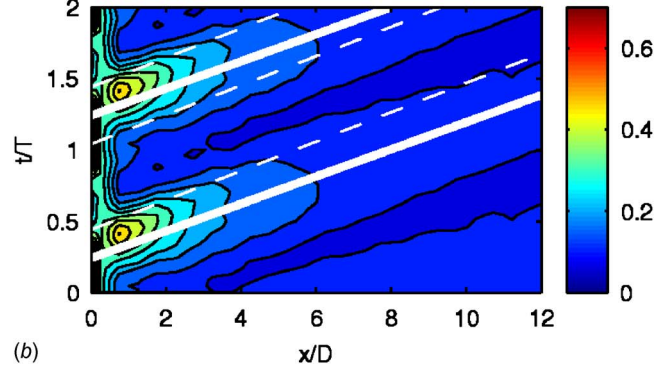


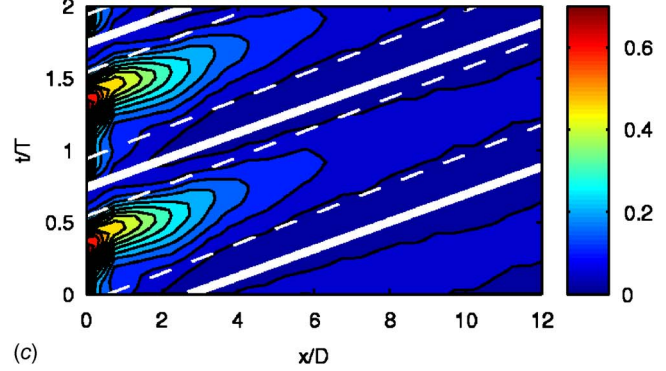
Fig. 23 Centerline Stanton number ratio,  $St_f/St_o$ , for  $B=1.0$ ,  $Sr=0.30$



(a)



(b)



(c)

Fig. 24 Phase averaged  $\eta^*$  for  $B=1.0$ ,  $Sr=0.60$ ; (a) P/NW, (b) P/WO, (c) P/WI

With  $B=1.0$ , the film cooling was dominated by jet lift-off. Pulsing reduced effectiveness by decreasing mass flow, but wakes tended to increase effectiveness somewhat by forcing more jet fluid closer to the wall, particularly near the film cooling holes.

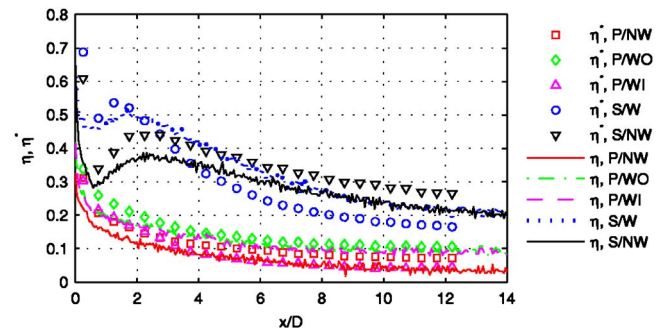


Fig. 25 Time averaged centerline  $\eta$  and  $\eta^*$  for  $B=1.0$ ,  $Sr=0.60$

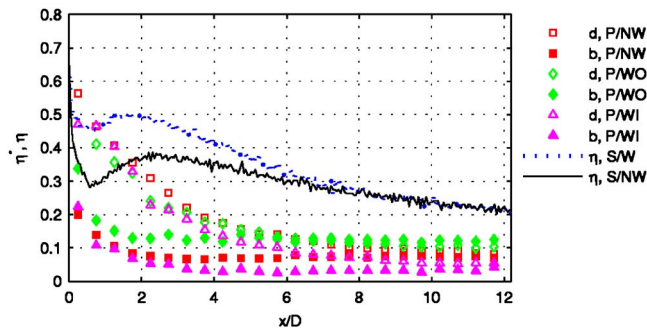


Fig. 26 Phase averaged centerline  $\eta^*$  for  $B=1.0$ ,  $Sr=0.60$  cases

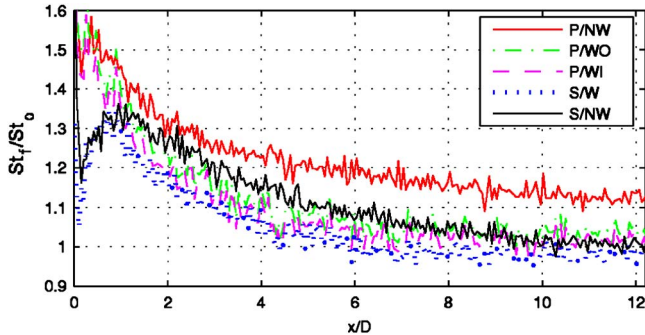


Fig. 27 Centerline Stanton number ratio,  $St_f/St_o$ , for  $B=1.0$ ,  $Sr=0.60$  cases

At low Strouhal numbers, the wake timing had a significant impact on the instantaneous film cooling effectiveness, but the effect of the wakes on the time averaged  $\eta$  was small. At higher Strouhal numbers, the wakes caused a greater reduction in time averaged effectiveness, but the shorter period of calm flow between wakes resulted in less variation during the cycle, thereby reducing the importance of wake timing. The time averaged effectiveness, therefore, did not depend strongly on wake timing at any Strouhal number.

Wakes caused a significant increase in heat transfer coefficient, but the effect was the same in cases with and without film cooling, and with all combinations of pulsing and wake timing. Stanton number ratios, therefore, showed no significant dependence on wake timing.

The present results indicate that there is no clear benefit to imposing pulsation on film cooling jets for the geometry considered. If pulsation occurs naturally in response to wakes, the present results provide some insight into how it affects the film cooling behavior.

### Acknowledgment

The first author gratefully acknowledges the Office of Naval Research for partial support of this work, via the Naval Academy Trident Scholar Program, on funding Document No. N0001406WR20137. The second author gratefully acknowledges partially support by the Naval Air Systems Command.

### Nomenclature

- $B = \rho_{jet} U_{jet} / \rho_{\infty} U_{\infty}$ , blowing ratio
- $c_p$  = specific heat at constant pressure
- $D$  = film cooling hole and wake generator rod diameter
- $f$  = frequency, Hz
- $L$  = length of film cooling hole channel
- $q''$  = heat flux

- $Sr$  = Strouhal number,  $Sr = 2\pi f D / U_{\infty}$
- $St$  = Stanton number,  $q''_{conv} / [\rho c_p U_{\infty} (T_w - T_{aw})]$
- $T$  = temperature or wake passing period
- $t$  = time
- $U$  = velocity
- $x$  = streamwise coordinate, distance from trailing edge of film cooling holes
- $y$  = normal coordinate, distance from the wall
- $z$  = spanwise coordinate, distance from the centerline of the center hole
- $\eta$  = film cooling effectiveness,  $(T_{aw} - T_{\infty}) / (T_{jet} - T_{\infty})$
- $\eta^*$  = approximate unsteady film cooling effectiveness, Eq. (3)
- $\rho$  = density
- $\phi$  = dimensionless temperature  $(T - T_{\infty}) / (T_{jet} - T_{\infty})$

### Subscripts

- aw = adiabatic wall
- conv = convective
- $f$  = with film cooling
- jet = film cooling jet
- $o$  = without film cooling, same wakes as corresponding  $f$  case
- w = wall
- $\infty$  = mainstream

### References

- [1] Ekkad, S. V., Ou, S., and Rivir, R. B., 2006, "Effect of Jet Pulsation and Duty Cycle on Film Cooling From a Single Jet on a Leading Edge Model," ASME J. Turbomach., **128**, pp. 564–571.
- [2] Funazaki, K., Yokota, M., and Yamawaki, S., 1997, "Effect of Periodic Wake Passing on Film Cooling Effectiveness of Discrete Cooling Holes Around the Leading Edge of a Blunt Body," ASME J. Turbomach., **119**, pp. 292–301.
- [3] Funazaki, K., Koyabu, E., and Yamawaki, S., 1998, "Effect of Periodic Wake Passing on Film Cooling Effectiveness of Inclined Discrete Cooling Holes Around the Leading Edge of a Blunt Body," ASME J. Turbomach., **120**, pp. 70–78.
- [4] Ou, S., Han, J. C., Mehendale, A. B., and Lee, C. P., 1994, "Unsteady Wake Over a Linear Turbine Blade Cascade With Air and CO<sub>2</sub> Film Injection: Part I—Effect on Heat Transfer Coefficients," ASME J. Turbomach., **116**, pp. 721–729.
- [5] Mehendale, A. B., Han, J. C., Ou, S., and Lee, C. P., 1994, "Unsteady Wake Over a Linear Turbine Blade Cascade With Air and CO<sub>2</sub> Film Injection: Part II—Effect on Film Effectiveness and Heat Transfer Distributions," ASME J. Turbomach., **116**, pp. 730–737.
- [6] Jiang, H. W., and Han, J. C., 1996, "Effect of Film Hole Row Location on Film Effectiveness on a Gas Turbine Blade," ASME J. Turbomach., **118**, pp. 327–333.
- [7] Ekkad, S. V., Mehendale, A. B., Han, J. C., and Lee, C. P., 1997, "Combined Effect of Grid Turbulence and Unsteady Wake on Film Effectiveness and Heat Transfer Coefficients of a Gas Turbine Blade With Air and CO<sub>2</sub> Film Injection," ASME J. Turbomach., **119**, pp. 594–600.
- [8] Du, H., Han, J. C., and Ekkad, S. V., 1998, "Effect of Unsteady Wake on Detailed Heat Transfer Coefficients and Film Effectiveness Distributions for a Gas Turbine Blade," ASME J. Turbomach., **120**, pp. 808–817.
- [9] Du, H., Ekkad, S. V., and Han, J. C., 1999, "Effect of Unsteady Wake With Trailing Edge Coolant Ejection on Film Cooling Performance for a Gas Turbine Blade," ASME J. Turbomach., **121**, pp. 448–455.
- [10] Teng, S., Sohn, D. K., and Han, J. C., 2000, "Unsteady Wake Effect on Film Temperature and Effectiveness Distributions for a Gas Turbine Blade," ASME J. Turbomach., **122**, pp. 340–347.
- [11] Teng, S., Han, J. C., and Poinatte, P. E., 2001, "Effect of Film-Hole Shape on Turbine-Blade Heat-Transfer Coefficient Distribution," J. Thermophys. Heat Transfer, **15**, pp. 249–256.
- [12] Teng, S., Han, J. C., and Poinatte, P. E., 2001, "Effect of Film-Hole Shape on Turbine-Blade Film-Cooling Performance," J. Thermophys. Heat Transfer, **15**, pp. 257–265.
- [13] Heidmann, J. D., Lucci, B. L., and Reshotko, E., 2001, "An Experimental Study of the Effect of Wake Passing on Turbine Blade Film Cooling," ASME J. Turbomach., **123**, pp. 214–221.
- [14] Wolff, S., Fottner, L., and Ardey, S., 2002, "An Experimental Investigation on the Influence of Periodic Unsteady Inflow Conditions on Leading Edge Film Cooling," ASME Paper No. GT-2002-30202.
- [15] Adami, P., Belardini, E., Montomoli, F., and Martelli, F., 2004, "Interaction Between Wake and Film Cooling Jets: Numerical Analysis," ASME Paper No. GT2004-53178.
- [16] Deinert, M., and Hourmouziadis, J., 2004, "Film Cooling in Unsteady Flow With Separation Bubble," ASME Paper No. GT2004-53075.
- [17] Womack, K. M., Volino, R. J., and Schultz, M. P., 2007, "Measurements in

Film Cooling Flows With Periodic Wakes,” ASME J. Turbomach., to be published.

- [18] Bons, J. P., Rivir, R. B., MacArthur, C. D., and Pestian, D. J., 1996, “The Effect of Unsteadiness on Film Cooling Effectiveness,” Wright Laboratory Technical Report No. WLTR-96-2096.
- [19] Ligrani, P. M., Gong, R., Cuthrell, J. M., and Lee, J. S., 1996, “Bulk Flow Pulsations and Film Cooling—I, Injectant Behavior, II. Flow Structure and Film Effectiveness,” *Int. J. Heat Mass Transfer*, **39**, pp. 2271–2292.
- [20] Seo, H. J., Lee, J. S., and Ligrani, P. M., 1999, “Effects of Bulk Flow Pulsations on Film Cooling From Different Length Injection Holes at Different Blowing Ratios,” ASME J. Turbomach., **121**, pp. 542–550.
- [21] Jung, I. S., Lee, J. S., and Ligrani, P. M., 2002, “Effects of Bulk Flow Pulsations on Film Cooling With Compound Angle Holes: Heat Transfer Coefficient Ratio and Heat Flux Ratio,” ASME J. Turbomach., **124**, pp. 142–151.
- [22] Ou, S., and Rivir, R. B., 2006, “Shaped-Hole Film Cooling With Pulsed Secondary Flow,” ASME Paper No. GT2006-90272.
- [23] Nikitopoulos, D. E., Acharya, S., Oertling, J., and Muldoon, F. H., 2006, “On Active Control of Film-Cooling Flows,” ASME Paper No. GT2006-90051.
- [24] Coulthard, S. M., Volino, R. J., and Flack, K. A., 2007, “Effect of Jet Pulsing on Film Cooling—Part 1: Effectiveness and Flowfield Temperature Results,” ASME J. Turbomach., **129**, pp. 232–246.
- [25] Coulthard, S. M., Volino, R. J., and Flack, K. A., 2007, “Effect of Jet Pulsing on Film Cooling—Part 2: Heat Transfer Results,” ASME J. Turbomach., **129**, pp. 247–257.
- [26] Burd, S., and Simon, T. W., 2000, “Effects of Hole Length, Supply Plenum Geometry, and Freestream Turbulence on Film Cooling Performance,” NASA Report No. CR-2000-210336.
- [27] Pedersen, D. R., Eckert, E. R. G., and Goldstien, R. J., 1977, “Film Cooling With Large Density Differences Between the Mainstream and the Secondary Fluid Measured by the Heat-Mass Transfer Analogy,” ASME J. Heat Transfer, **99**, pp. 620–627.
- [28] Kohli, A., and Bogard, D. G., 1998, “Fluctuating Thermal Field in the Near-Hole Region for Film Cooling Flows,” ASME J. Turbomach., **120**, pp. 86–91.
- [29] Coulthard, S. M., Volino, R. J., and Flack, K. A., 2006, “Effect of Unheated Starting Lengths on Film Cooling Experiments,” ASME J. Turbomach., **128**, pp. 579–588.